Available online at www.sciencedirect.com
ScienceDirect
Journal of Power Sources 158 (2006) 1262–1269
JOURNAL OF POWER SOURCES
www.elsevier.com/locate/jpowsour

Some anion-transport properties of Nafion™ 117 from fuel cell hydrogen peroxide generation data

Piotr Piela *, Piotr K. Wrona

Industrial Chemistry Research Institute, Rydygiera 8, 01-793 Warsaw, Poland

Received 23 June 2005; received in revised form 27 September 2005; accepted 10 October 2005
Available online 15 November 2005

Abstract

Hydrogen peroxide generation R&D data obtained in an alkaline fuel cell-type electrochemical reactor with a dividing Nafion™ 117 membrane have been used to extract anion-conducting properties of the cation-exchange membrane. The effective diffusion coefficient of NaOH and the average transport number of OH^- in the membrane were obtained by fitting a model formula for the total alkalinity of outlet catholyte to experimental alkalinities obtained with various electrolysis parameters' values. The formula resulted from assumptions that NaOH diffuses through the membrane and OH^- migrates through the membrane, and that HO_2^- does not penetrate the membrane. The membrane parameters extracted in this way were in good agreement with similar data reported by others for Nafion™. Hydrogen peroxide current efficiencies remained over 90% and H_2O_2 concentrations reached 7 wt.%, however the fuel cell reactor's electrical efficiency was strongly limited by high internal resistance.

Keywords: Hydrogen peroxide; Fuel cell; Nafion™; Diffusion coefficient; Transport number; Oxygen reduction

1. Introduction

Nafion™ is by far the most studied polymeric electrolyte, because of its high ionic conductivity and chemical resistance. It is widely used in fuel cell research, e.g. [1–3], and in electrosynthesis, mainly chlor-alkali, e.g. [4], where it should act as a selective cationic (H^+ or Na^+ conductor). The ionic conductivity of Nafion™ strongly depends on the degree of hydration of the polymer, the temperature, and the cationic form the polymer is in, with the two latter factors influencing the first factor. For this reason, the important type of investigations of Nafion™ was to determine its ion-transport properties, i.e. the diffusion coefficients and transport numbers of various ions in the polymer, and to propose a suitable mechanism of ionic conduction.

In the case of ionomer membranes, which are the usual geometric forms of Nafion™, the transport parameter easiest to obtain is the permeation coefficient. It is the coefficient of combined diffusion of both the anion and the cation of an electrolyte in the membrane. It is equivalent to the apparent diffusion coefficient of a salt in a liquid. To obtain this parameter it is enough to determine the difference of concentrations of the electrolyte in the membrane on both sides of it (the driving force) and the simultaneous flux of the electrolyte across it (the effect). When the partition coefficient of the electrolyte between the membrane and contacting solution, defined as the ratio of the concentration in the membrane-absorbed solution to that in the membrane-contacting solution, is unknown, only the effective permeation coefficient is accessible. This coefficient is based on the concentrations of the membrane-contacting solutions. An example for HCl and Nafion™ 117 is found in [5] and for HCl, NaCl, and KCl and various membranes in [6].

A more fundamental property of the ionomer and ion is the self-diffusion coefficient of the ion in the ionomer. To determine this property a number of methods have been proposed. The most established method is the radiotracer method, which is based on radioactivity measurements of the ionomer contacted with a solution of the radiolabeled ion. There are modifications of this basic method, in which the authors seek to obtain well-defined boundary conditions for diffusion [7,8]. These methods provide the so-called "true" self-diffusion coefficients, because the total activity of the ion in the ionomer is kept constant and the isotopic effect in diffusion is believed to be negligible for ions larger than the proton. Ion-exchange measurements can also yield this parameter. In this type of measurement unlabeled

* Corresponding author. Tel.: +48 22 568 2908; fax: +48 22 568 2390.
E-mail address: piotr.piela@ichp.pl (P. Piela).

0378-7753/$ – see front matter © 2005 Elsevier B.V. All rights reserved.
doi:10.1016/j.jpowsour.2005.10.019

Nomenclature

A	working cross-section area of the reactor (cm^2)
$C^{tot}_{c,out}$	total outlet alkalinity of catholyte ($mol\ dm^{-3}$)
$C_{HO_2^-}$	molar concentration of hydrogen peroxide in product catholyte ($mol\ dm^{-3}$)
$C_{HO_2^-,theor}$	molar concentration of hydrogen peroxide in product catholyte when $\Phi = 1$ ($mol\ dm^{-3}$)
C^y_x	concentration of species y at place x ($mol\ dm^{-3}$)
d	membrane thickness (cm)
D	effective diffusion coefficient of NaOH diffusion in the membrane ($cm^2\ s^{-1}$)
E^0	standard redox potential (V)
F	Faraday's constant ($C\ mol^{-1}$)
I	reactor's current (A)
n^y_x	stream of species y at place x ($mol\ min^{-1}$)
Δn^y_m	production of species y according to mechanism m ($mol\ min^{-1}$)

Greek letters

Φ	current efficiency for hydrogen peroxide
ν_a	volumetric velocity of anolyte at anolyte outlet ($cm^3\ min^{-1}$)
ν_c	volumetric velocity of catholyte at catholyte outlet ($cm\ min^{-1}$)
τ	average transport number for OH^- in the membrane

ions are exchanged between solution and ionomer. The analysis involves always at least two different ions. From such experiments, based on an observed correlation between the ratio of the diffusion coefficient in the membrane and in solution and the liquid volume fraction of the membrane, it was concluded [9,10] that fully hydrated Nafion^{TM} membranes are simply steric barriers to the ions. A further method is based on ionomer conductivity measurement. It was shown, however, that the mobility of ions assessed from conductivity extrapolated to zero net current is importantly higher than the one obtained from radiotracer methods [11]. This discrepancy, also present in the case of concentrated solutions, is explained in terms of particularly strong electrophoretic effects due to the interaction of free ions with the fixed ionic sites inside the ionomer and with each other in ionomer channels of small diameter. There are also more sophisticated methods to study diffusion in confined media. In the quasi-elastic neutron scattering [12] the diffusion of ions can be observed at time scales below 1 ps. Pulsed-field NMR [13] is used to study diffusion on time scales from below 1 s to tens of seconds. It was shown [14,15] that at the shortest observation times the values of the self-diffusion coefficients of ions in Nafion^{TM} approach those in solution. As the time of observation gets longer these values start to depend on the concentration of ions in the ionomer. At the longest times of observation (radiotracer method) this dependence becomes weaker.

The transport number for individual ions in ionomers is accessible through electrochemical experiments. In the cases, when it was established for Nafion^{TM} it turned out that the charge is almost uniquely carried by the counter ion, i.e. the cation [5,6]. The only exception is the case when OH^- is the anion of the liquid electrolyte employed in experiments of this type. Because of an efficient proton-hopping transport mechanism for OH^- (the Grøtthus mechanism), the cation transport number can be significantly lower than unity when OH^- is the co-ion [16].

From these and other observations (e.g. conductivity versus hydration, or microscopy) an image of the Nafion^{TM} structure was built. It should be considered a network of liquid-filled pores in which the walls of the pores are decorated with fixed SO_3^- sites. The size of the pores depends on the water content of the ionomer and is such that the counter-ions moving in the pores can "feel" the presence of the fixed sites to an extent dependent on the amount of soaked water. This situation corresponds to pores of ca. 5 nm mean diameter for typical Nafion^{TM} 1100 e.w. membrane material in fully hydrated form. Modeling of structures of this type is an ongoing effort. The Brownian mechanics approach was presented in [14]. A non-equilibrium statistical mechanical model for proton conduction was introduced in [17]. A molecular dynamics simulation of the structure of water-swollen Nafion^{TM} was presented in [18].

In the present work, we were able to determine a strong ability of fully hydrated, sodium-form Nafion^{TM} 117 to carry the hydroxide anion in preference to the hydroperoxide anion—a feature that could be used to the advantage of an alkaline hydrogen peroxide generation process. The effective sodium hydroxide permeation coefficient and the average OH^- transport number in the membrane, determined by us at different temperatures, as well as the simple method of extracting those parameters, might be of interest to the developers of the chlor-alkali process, where the membranes also operate under mixed Na^+/OH^- conduction.

The results presented here were obtained as part of the efforts conducted at the Industrial Chemistry Research Institute to develop an electrochemical reactor for the production of hydrogen peroxide, particularly an alkaline fuel cell-type reactor for the production of an alkaline solution of hydrogen peroxide, at little expense for, no expense, or with a gain of energy from the process. It is known that molecular oxygen can be efficiently reduced to hydrogen peroxide in the alkaline medium on a small number of electrode materials, namely mercury, gold and graphite [19]. Graphite is the technological material of choice, because of cost and environmental protection issues. The idea of a suitable electrochemical reactor is depicted in Fig. 1. The device uses a carbon-only gas-diffusion cathode to reduce gaseous oxygen to hydroperoxide anions according to the reaction:

$$O_2 + H_2O + 2e \rightarrow HO_2^- + OH^-, \quad E^0 = -0.076\,V \qquad (1)$$

and a gas-diffusion anode with platinum catalyst to oxidize gaseous hydrogen to water:

$$H_2 + 2OH^- \rightarrow 2H_2O + 2e, \quad E^0 = -0.828\,V \qquad (2)$$

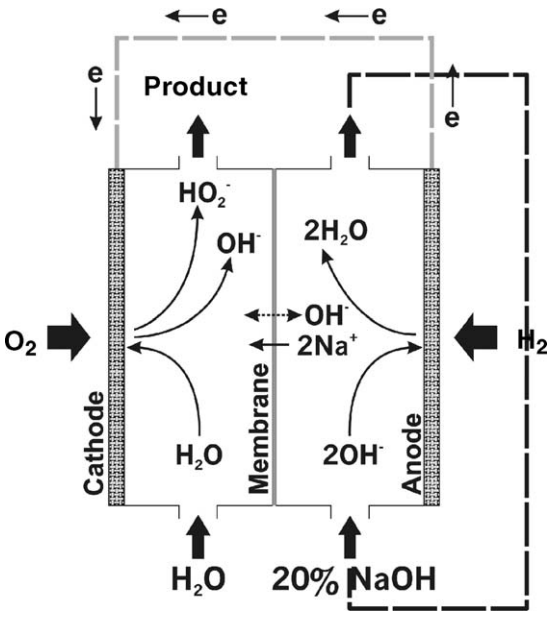

Fig. 1. Concept scheme of alkaline hydrogen peroxide generation in fuel cell-type reactor.

Because of complications of reaction (1) [20], namely disproportionation of HO_2^-:

$$2HO_2^- \rightarrow O_2 + 2OH^- \quad (3)$$

and (less probable on carbon) electro-reduction of HO_2^- at the cathode:

$$HO_2^- + H_2O + 2e \rightarrow 3OH^-, \quad E^0 = 0.867\,V \quad (4)$$

the overall cathode process is described in terms of the current efficiency for hydrogen peroxide, Φ, taking values from 0 to 1:

$$(1/2)(\Phi + 1)O_2 + H_2O + 2e \rightarrow \Phi HO_2^- + (2 - \Phi)OH^-,$$
$$E^0\,(V) = 0.401\text{–}0.477\Phi \quad (5)$$

The overall process in the reactor is

$$(1/2)(\Phi + 1)O_2 + H_2 + \Phi OH^- \rightarrow \Phi HO_2^- + H_2O \quad (6)$$

The standard free Gibbs energy of reaction (6) is $(-237.2 + 92.0\Phi)\,kJ\,mol^{-1}$, hence the process can be operated such that the reactor will be a source of electricity—a fuel cell.

An important part of the reactor is a cation-exchange membrane dividing it into the cathode (product) and the anode compartments. The purpose to use the membrane is to prevent HO_2^- ions from reaching the anode, where they would be inevitably lost in reactions (3) and (4) because of the electrochemical conditions prevailing there (negative potential and presence of metallic catalyst). Also, the membrane plays a role in the control of the ratio of sodium hydroxide to hydrogen peroxide in the product liquor. This ratio should be kept at a minimum, because of the requirements of the pulp bleaching processes, where the liquor is to be used. The membrane allows using water as the incoming catholyte (for a theoretical treatment of this case see [21]), thus the sodium hydroxide present in the product comes only from the processes inside the reactor. Apart from these functions, all the other membrane influence on the process is unwanted. The presence of membrane raises the internal resistance of the reactor and adds to its complexity and cost. Needless to say, the ion transport properties of the membrane have a direct impact on the current efficiency, Φ, the composition of product, and the electrical performance of the reactor. By doing the balance of species for the reactor we were able to determine some of these properties.

A second purpose of this contribution is to present the concept of hydrogen peroxide fuel cell generator at work. Although for full commercial viability additional R&D is needed, the results obtained so far reveal strong potential of this method and indicate the direction for future R&D.

2. Experimental

The idea of the hydrogen peroxide fuel cell-type reactor shown in Fig. 1 was embodied in a single cell employing the typical parallel plate and frame design. The oxygen cathode was a specialty carbon-only gas-diffusion electrode and the hydrogen anode was an ELAT gas-diffusion electrode with 20% Pt on Vulcan XC-72 carbon black catalyst and a Pt loading of $0.40\,mg\,cm^{-2}$, both from E-TEK, Inc. (USA). The electrodes were contacted with 100%-nickel mesh current collectors. Each electrode's working geometric area was $66.3\,cm^2$. The cathode and the anode liquid compartments were separated with a Nafion^{TM} 117 membrane (Du Pont, USA). The compartments were filled with expanded PVC spacers, which provided for compression of the gas-diffusion electrodes to the current collectors and for holding the membrane straight between the compartments. The plates and frames forming the body of the fuel cell were made of poly(methyl methylacrylate). Silicone rubber gaskets assured cell sealing.

The reactor was operated in a laboratory installation presented in Fig. 2. The cathode liquid compartment was fed with preheated deionized water by means of a precision peristaltic pump and the anode compartment was fed with preheated 20 wt.% NaOH (p.a., from POCh S.A., Poland) in deionized water by means of a heavy-duty chemical-resistant membrane pump (Cole-Partner, USA). The anolyte was re-circulated from a tank, in which the depleting concentration of NaOH was frequently readjusted to 20 wt.%. Pure pre-humidified oxygen was fed to the cathode and pure pre-humidified hydrogen was fed to the anode (both from Multax SC, Poland). A slight backpressure of both gases was maintained with the use of tall liquid closures placed at the outlets of the gas lines.

The fuel cell reactor was polarized with a Hewlett-Packard 6031A system power supply coupled with an Agilent 6051A/60504B dc electronic load. Both instruments were controlled with a personal computer running in-house data acquisition software. The software allowed for recording constant voltage/current/resistance polarization data as well as automatic steady-state polarization curve recording. The steady-state polarization curves were acquired in constant current mode. The steady-state voltage value for a given applied current value was recorded when the monitored voltage changed no more than $0.5\,mV\,min^{-1}$ at the end of a walking 20-s observation

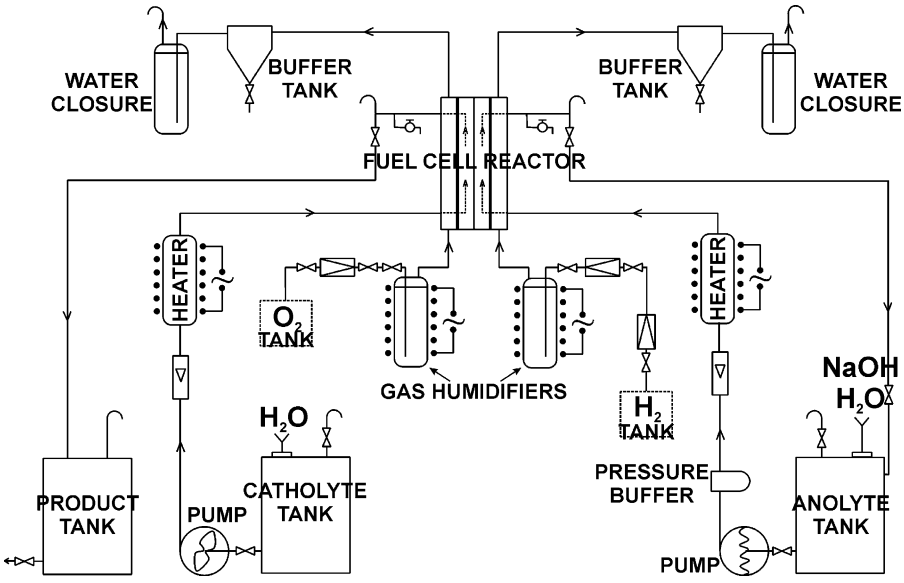

Fig. 2. Scheme of laboratory installation for alkaline hydrogen peroxide.

window (parabola fitting to last 20 measurements taken at 1 s intervals).

The concentration of hydrogen peroxide was determined spectrophotometrically in samples of the catholyte leaving the reactor using a procedure based on the reaction of HO_2^- with $K_3[Fe(CN)_6]$ in alkaline solution, which is described elsewhere [22]. The total alkalinity of the product catholyte was determined by potentiometric titration with sulfuric acid. Since no peroxide was found in the anolyte leaving the reactor, the hydrogen peroxide current efficiency was determined from the concentration of peroxide in the product catholyte according to the formula:

$$\Phi = \frac{C_{HO_2^-}}{C_{HO_2^-,\mathrm{theor}}} = 3.33 \times 10^{-5} \frac{F v_c C_{HO_2^-}}{I} \tag{7}$$

This formula requires the catholyte sample for peroxide determination to be collected after a time from start of electrolysis sufficient to push at least one dead volume of the catholyte chamber through that chamber.

3. Determination of anion-conducting properties of the membrane

As it will be obvious from Section 4, one could not assume that the Nafion™ 117 membrane was 100% cation-selective in the studied system. On the other hand, the peroxide anion seemed not to penetrate the membrane significantly. Therefore, a model for the balance of species in the reactor was assumed, according to which the membrane can be crossed by Na^+ and OH^-, but not HO_2^- species (cf. Fig. 1). Let us focus on the total alkalinity of outlet catholyte. It is obvious that three factors influenced it: (i) faradaic production of HO_2^- and OH^- at the fuel cell cathode, (ii) diffusion of NaOH through the membrane in the direction opposite to the NaOH concentration gradient across the membrane, and (iii) migration of OH^- through the membrane in the direction opposite to the current. Because the fuel cell reactor is a flow-through device, in which the catholyte and anolyte flow in channels defined by the respective electrode, the membrane and the acrylic frame, calculation of the total alkalinity would require at least 2D modeling of transport of species in the reactor's flow channels and the membrane. Even in the case of a simplest pseudo-2D model assuming only forced convection as a transport mechanism along the channels (no diffusion and migration) the description of the alkalinity can be arrived at only by numerical simulation. In order to extract membrane properties from experimental data one would have to fit such a numerical model to the data. All in all, extensive programming would be inevitable and usefulness limited. Moreover, correctness of this sort of model would remain questionable regardless of the level of sophistication. However, the purpose of the present modeling is to show a simple method of extracting membrane properties from reactor's data. As it turns out, it can be done by making only one and justified assumption: the concentration of all species at the outer surfaces of the membrane is approximately linear with the distance along the length of the flow channels. Upon this assumption, the balance of species needs to be done only for average concentrations, i.e. the concentrations halfway along the flow channels. We now present the simple balance equations.

The total outlet alkalinity of catholyte is

$$C_{c,\mathrm{out}}^{\mathrm{tot}} = C_{c,\mathrm{out}}^{OH^-} + C_{HO_2^-} = \frac{1000}{\nu_c}(n_{c,\mathrm{out}}^{OH^-} + n_{c,\mathrm{out}}^{HO_2^-}) \tag{8}$$

Because HO_2^- is electrogenerated only (no membrane crossing, no supply with inlet streams), its outlet stream is given by

$$n_{c,\mathrm{out}}^{HO_2^-} = 60\frac{I\Phi}{2F} \tag{9}$$

The cathode compartment is always supplied with deionized water only, therefore, the catholyte outlet stream of OH^- is the

result of faradaic production of OH^- at the cathode and transport of OH^- through the membrane via diffusion and migration mechanisms:

$$n_{c,out}^{OH^-} = \Delta n_{farad}^{OH^-} + \Delta n_{diff}^{OH^-} + \Delta n_{migr}^{OH^-} \quad (10)$$

The three Δn components are given by

$$\Delta n_{farad}^{OH^-} = 60\frac{I(2-\Phi)}{2F} \quad (11)$$

$$\Delta n_{diff}^{OH^-} = 0.06AD\frac{0.5(C_{a,in}^{OH^-} + C_{a,out}^{OH^-} - C_{c,out}^{OH^-})}{d} \quad (12)$$

$$\Delta n_{migr}^{OH^-} = -60\frac{I\tau}{F} \quad (13)$$

Eqs. (11)–(13) make use of the simplifying assumption about linearity of concentrations with distance along the flow channel.

Combining Eqs. (8) through (13) we can express the total outlet alkalinity of catholyte in terms of $C_{a,in}^{OH^-}$, $C_{a,out}^{OH^-}$, Φ, A, d, F, I, ν_c, D, and τ. The resulting equation is not given here, because of its bulkiness. Furthermore, $C_{a,out}^{OH^-}$ can be expressed in terms of the other quantities in the list plus ν_a by doing the balance of OH^- for the whole reactor involving the total NaOH input to the reactor with the incoming anolyte and the electrochemical production (cathode) and consumption (anode) of OH^- in the reactor. Hence, the ultimate list of parameters $C_{c,out}^{tot}$ depends on contains only two unknown parameters: D and τ. The other ones are known (A, d, F) or set/found in the course of the experiment ($C_{a,in}^{OH^-}$, Φ, I, ν_c, ν_a). Again, the full formula is too large to be shown here and is in itself of little interest.

Parameters D and τ are of interest, because they reflect the anion transport properties of the Nafion™ 117 membrane. In order to extract them, a set of electrolysis experiments was performed, in which I and ν_c were varied with the other adjustable parameters left constant. For every pair of I and ν_c values, experimental $C_{c,out}^{tot}$ as well as Φ were determined. We were able to find parameters D and τ for different operating temperatures by non-linear least-squares fitting of the formula for $C_{c,out}^{tot}$ to its experimental values, with parameters D and τ being the adjustable parameters of the fit.

4. Results and discussion

Fig. 3 presents the steady-state polarization curve of the fuel cell reactor. The open circuit voltage of the reactor was ca. 0.810 V. This value is a little higher than the voltage calculated from standard potentials of reactions (1) and (2) (0.752 V). Assuming these reactions fixed reactor electrodes' potentials and taking into account the close-to-standard conditions prevailing in the reactor,[1] one would expect the open circuit voltage to be very close to the mentioned difference of standard potentials.

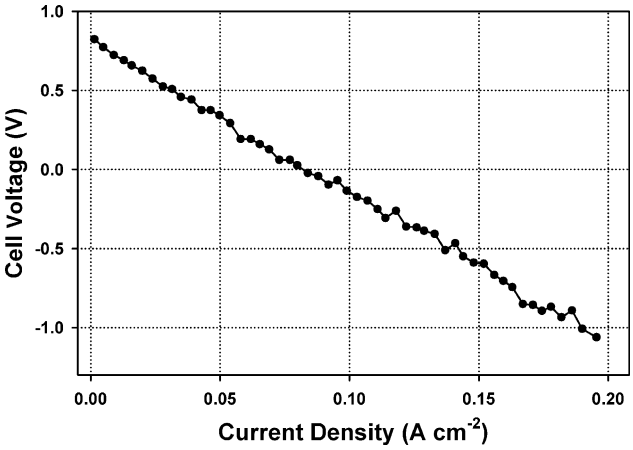

Fig. 3. Stationary polarization curve of single cell reactor (current-driven). Working cross-section: 66.3 cm^2, incoming anolyte: 20 wt.% NaOH at 10 $cm^3\ min^{-1}$, incoming catholyte: deionized water at 1.5 $cm^3\ min^{-1}$, operating temperature: 50 °C, O_2 feed: humidified at 50 °C, back-pressurized to 45 cm of water, 300 ($m^3\ min^{-1}$ (STP) H_2 feed: humidified at 50 °C, back-pressurized to 25 cm of water, 300 ($m^3\ min^{-1}$ (STP).

An explanation of the higher voltage can be such that the cathode reaction was slightly shifted towards four-electron oxygen reduction to OH^- by the occurrence of reaction (3). Thus, cathode potential and, consequently, cell voltage were increased.

In the cell voltage region from the open circuit voltage down to 0 V, i.e. up to the current density of ca. 80 mA cm^{-2}, the reactor produced electrical energy. Below 0 V, i.e. for higher demanded current densities, energy had to be supplied to the reactor, because of polarization losses. It is interesting that the polarization curve was an almost perfect straight line in the whole range of studied current densities. Also, when we would reverse the direction of current, the line would continue from open circuit voltage up, without change of slope (data not shown). All this suggests that: (i) a single electrochemical reaction step occurred at the cathode in the current density range studied, (ii) both electrode reactions were reversible or close to this state, (iii) the electrical performance of the fuel cell reactor was limited chiefly by ohmic losses, and (iv) mass transport limitations were negligible even for the highest current densities studied. Conclusions (ii)–(iv) open a clear pathway to improvement of the electrical performance: the internal resistance of the reactor has to be lowered by adequate reactor design. In fact, the margin for improvement is substantial, because the internal resistance for the present reactor was ca. 10 Ω cm^2, i.e. almost two orders of magnitude more than the values for typical energy-producing fuel cells.

Fig. 4 shows the change of the hydrogen peroxide current efficiency in the course of a two-week uninterrupted life test of the fuel cell reactor at a constant current density of 0.100 A cm^{-2}. We can see that after initial adjustment of process parameters during the first 100 h Φ remained on average at a level of 0.93 with no sign of degradation. Combined with conclusions from Fig. 3, this indicates that the cathode electrochemical step was indeed reaction (1). Besides, HO_2^- seems not to have penetrated the membrane substantially or decomposed according to reaction (3) in the cathode chamber. In order to achieve the latter,

[1] The only exception was pH, however both anolyte pH was 14 and catholyte pH at open circuit was also close to 14 due to Nafion™ 117 being a leaking membrane, as seen below. Since, both the cathode and the anode potentials shift by the same amount of mV for a unit change of pH, their difference, i.e. the voltage at pH 14 and at standard pH 0 should be the same.

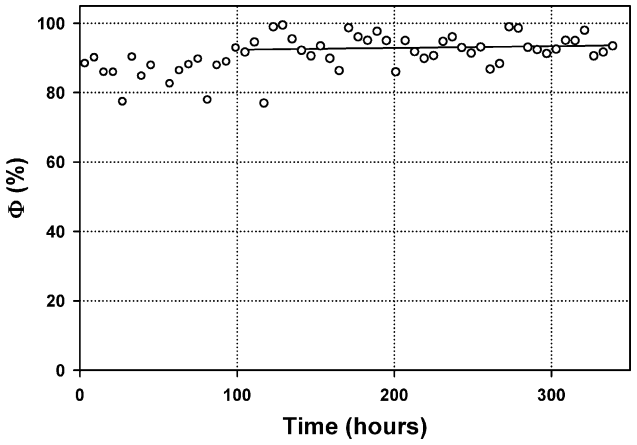

Fig. 4. Hydrogen peroxide current efficiency over 2-week uninterrupted operation of fuel cell reactor at 0.100 A cm^{-2} Product concentration was tuned to different values in the range 3.5–5.0 wt.% H_2O_2. Operating temperature: 45–60 °C; incoming anolyte: 20 wt.% NaOH at 10 cm^3 min^{-1}; incoming catholyte: deionized water; O_2 feed: humidified at 50 °C, back-pressurized to 45 cm of water, 2× stoichiometric; H_2 feed: humidified at 50 °C, back-pressurized to 25 cm of water, 2× stoichiometric.

especially with relatively high concentrations of product peroxide, special care must be taken to avoid or block catalytic impurities in the system.

A set of electrolysis experiments was performed with varying I and v_c in order to extract membrane properties, as explained earlier. The total alkalinity of the resulting catholyte is plotted in Fig. 5 (filled circles). The same figure contains values of total alkalinity predicted from I and v_c with the assumption of 100% selectivity of the Nafion™ 117 membrane towards cations (open circles). One can see that for small current densities and small velocities of catholyte, the catholyte was excessively alkaline, whereas in the opposite situation, particularly for high current densities, the catholyte had less NaOH than expected merely from cathodic production. Additionally, the mentioned differences could be large indicating strong anion-leaking properties of the membrane. These leaking properties of the membrane are beneficial, because by adjusting the current density and catholyte velocity we can obtain a product with a small hydroxide-to-peroxide ratio, i.e. one that is desired by the pulp and paper industry—the target industry for this technology.

The peroxide current efficiencies for the set of electrolysis data from Fig. 5 are presented in Fig. 6. Fig. 6a is a projection of the 3D plot to reveal the dependence of Φ on the current density. Although a variation of efficiency was observed, it is important to note that there was no strong dependence in the wide range of current densities shown. In other words, high current was not

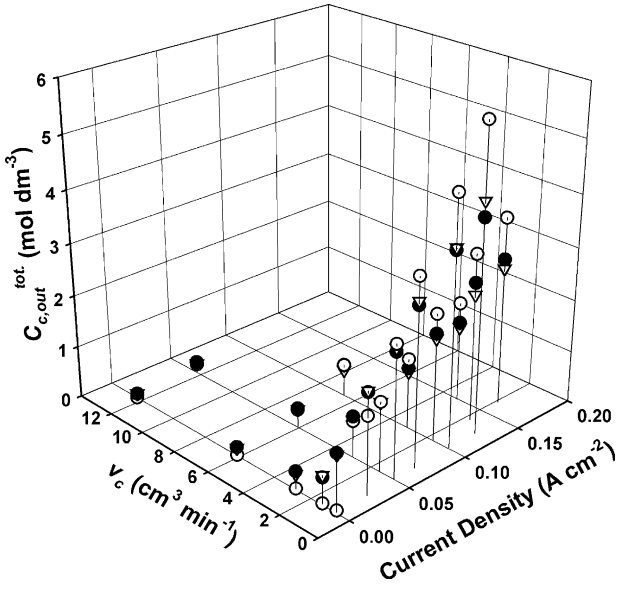

Fig. 5. Total alkalinity of product liquor vs. current density and catholyte volumetric flow rate: (filled circles) from titration after 2-h operation at fixed current density and catholyte volumetric flow rate, (empty circles) expected at no OH^- crossing the membrane, (triangles) predicted from NaOH diffusion and OH^- migration through membrane. Operating temperature: 50 ± 3 °C; other parameters as for Fig. 4.

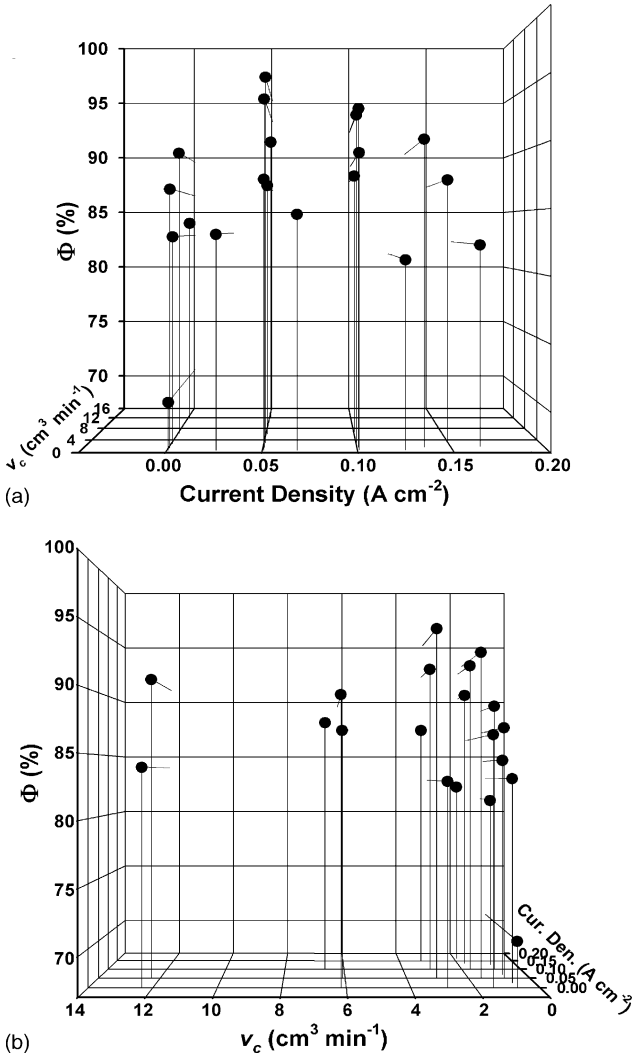

Fig. 6. Hydrogen peroxide current efficiency vs. current density and catholyte volumetric flow rate: (a) projection to reveal influence of current density and (b) projection to reveal influence of catholyte volumetric flow rate. Operating parameters as for Fig. 5.

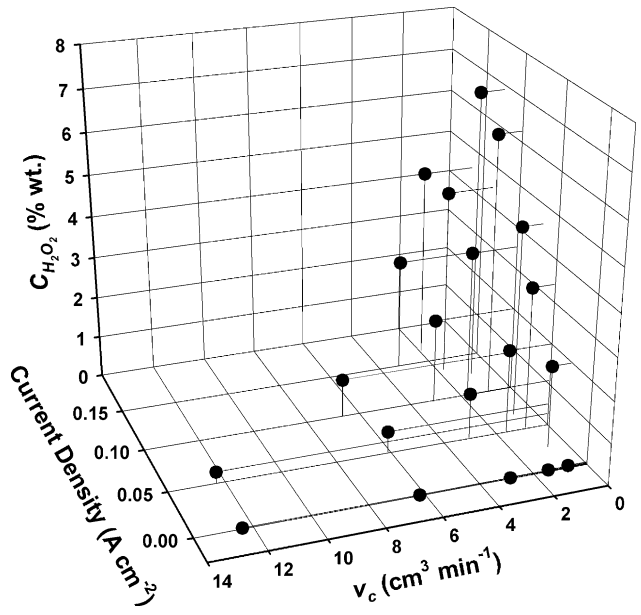

Fig. 7. Concentration of hydrogen peroxide in product liquor vs. current density and catholyte volumetric flow rate. Operating parameters as for Fig. 5.

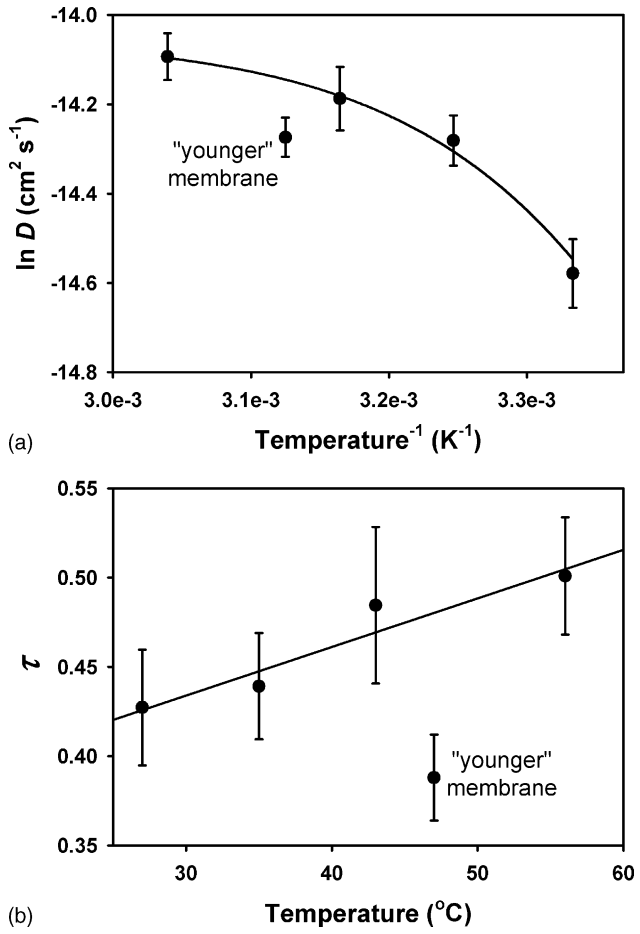

Fig. 8. Influence of temperature on (a) average effective diffusion coefficient of NaOH and (b) average transport number of OH^- in the Nafion^{TM} 117 membrane. Bars indicate parameter errors from fitting.

leading to a substantial loss of HO_2^-. Similarly, Fig. 6b is a projection to reveal the dependence of Φ on ν_c. Again, there was no strong dependence, which particularly indicates that long reactor residence time of HO_2^- was not leading to its decomposition or loss through the membrane. Fig. 6 is, therefore, evidence that the assumptions about HO_2^- done for the balance of species in the reactor were justified (see earlier). Fig. 7 shows the steady peroxide concentrations obtained for each electrolysis experiment expressed as the H_2O_2 weight percent. The most concentrated product catholyte obtained was almost 7 wt.% H_2O_2 ($\Phi = 0.91$). Figs. 6 and 7 demonstrate the practical value of the fuel cell reactor.

The total alkalinity of outlet catholyte from Fig. 5 was fitted with the formula obtained assuming diffusion of NaOH and migration of OH^- through the membrane, as described earlier. Fig. 5 contains predicted alkalinity values obtained from the fit (triangles). As can be seen from the figure, those values lie very close to the experimental values (filled circles) virtually for every I and ν_c. This result supports correctness of the proposed membrane behavior with respect to OH^- and HO_2^-.

The fit yielded D and τ for the particular operating temperature of the reactor/membrane. We have conducted such electrolysis experiments for a number of temperatures. The resulting D and τ values are presented in Fig. 8. The values of D obtained here are in agreement of order with the values obtained by other authors for Nafion^{TM} 117 and, e.g. HCl [5] and various ions [6,7,11,14]. Fig. 8a is an attempt to analyze the D parameter in Arrhenius coordinates, since it is known that diffusion typically behaves as an activation process. Although D increased with temperature, no straight line was obtained in the Arrhenius plot. It must be borne in mind, however, that we have studied here a process of substance permeation through a thin porous medium with a tendency to swell on contact with liquid water according to temperature, rather than typical Brownian motion diffusion. Two factors can play a role in such system: (i) the usual, i.e. increase of ionic mobility with temperature and (ii) closing/expansion of the pores plus changes of their tortuosity upon swelling. As to τ, its value also slightly increased with temperature. It can be assumed that the swelling also caused this effect. The increase of distance between the sulfonic anion groups of Nafion^{TM} and OH^- that accompanies swelling should lead to less repulsion and increased share of OH^- in conduction through the membrane.

Fig. 8 also contains a data point obtained for a membrane that was freshly mounted in the reactor and hydrated for 24 h prior to the series of electrolysis experiments. One can see that the anion permeability of this "fresh" membrane was lower than that of a membrane working in the reactor for a long time (ca. a month prior to electrolysis experiments). This indicates that the Nafion^{TM} 117 membrane material working in the strong alkaline environment of the fuel cell reactor undergoes a slow and irreversible transformation process probably associated with increase of the nanopores' diameters in the polymer. As mentioned earlier, Nafion^{TM} polymer is known for strong swelling on contact with water, which is explained in terms of enlargement of

the liquid water plenum in the structure of the hydrophilic polymer accompanied by increase of the average distance between polymer fibers and, consequently, increase of the fluid channels (nanopores). The process of water uptake under mild conditions is generally reversible, i.e. the polymer regains most of its pre-swelling structure after drying. However, when harsh conditions are used, e.g. elevated temperature and pressure plus alcohol solvents, the structure of the solid polymer breaks irreversibly and a suspension of particles ultimately forms. It is therefore possible that a slow, irreversible structure degradation of Nafion^{TM} takes place also under mild swelling conditions leading to increased overall permeability of the polymer.

5. Conclusions

We have presented hydrogen peroxide generation R&D data obtained in an alkaline fuel cell-type electrochemical reactor that possessed a dividing Nafion^{TM} 117 membrane. The reactor's data could be used to extract anion-conducting membrane properties of the cation-exchange membrane. The simple way to extract those properties, namely the effective diffusion coefficient of NaOH and the average transport number of OH^-, consisted of fitting a model formula for the total alkalinity of outlet catholyte to experimental alkalinities obtained with various electrolysis parameters' values. The formula resulted from assumptions that NaOH diffuses through the membrane and OH^- migrates through the membrane, and that HO_2^- does not penetrate the membrane. Validity of these assumptions was confirmed by constantly high current efficiency of peroxide generation and by good fitting results. The membrane parameters extracted by fitting were in good agreement with similar data reported for Nafion^{TM}. The fuel cell reactor's electrical efficiency appeared to be limited by high internal resistance. Vis-à-vis high peroxide current efficiencies (>90%) and peroxide concentrations (up to 7 wt.%, H_2O_2 basis) obtained in the reactor, lowering of the internal resistance could lead to a viable technology for on-site generation of peroxide bleach targeted at the pulp and paper industry.

Acknowledgments

The Polish Ministry of Science financially supported this work through grant no. 3 T09B 055 29 awarded for the years 2005–2007.

References

[1] A.J. Appleby, in: I.O. Savadogo, P.-R. Roberge, T.N. Veziroğlu (Eds.), New Materials for Fuel Cell Systems, Éditions de l'École Polytechnique de Montréal, Montreal, 1995, pp. 2–35.
[2] S. Srinivasan, J. Electrochem. Soc. 136 (1989) 41C.
[3] P. Piela, P. Zelenay, Fuel Cell Rev. 1 (2004) 17.
[4] T. Asawa, J. Appl. Electrochem. 19 (1989) 566.
[5] G. Schwitzgebel, F. Endres, J. Electroanal. Chem. 386 (1995) 11.
[6] S. Koter, P. Piotrowski, J. Kerres, J. Membr. Sci. 153 (1999) 83.
[7] A.L. Rollet, J.P. Simonin, P. Turq, Phys. Chem. Chem. Phys. 2 (2000) 1029.
[8] A. Goswami, A. Acharya, A.K. Pandey, J. Phys. Chem. B 105 (2001) 9196.
[9] Z. Samec, A. Trojanek, E. Samcova, J. Phys. Chem. 98 (1994) 6352.
[10] Z. Samec, A. Trojanek, J. Langmaier, E. Samcova, J. Electrochem. Soc. 144 (1997) 4236.
[11] G. Pourcelly, P. Sistat, A. Chapopot, C. Gavach, V. Nikonenko, J. Membr. Sci. 110 (1996) 69.
[12] M. Bée, Quasi-Elastic Neutron Scattering: Principles and Applications in Solid State Chemistry, Biology and Materials Science, Adam Hilger Ed., Bristol, 1988.
[13] C.S. Johnson Jr., in: D.M. Grand, R.K. Harris (Eds.), Encyclopedia of NMR, Wiley, New York, 1996, pp. 1626–1644.
[14] A.-L. Rollet, J.-P. Simonin, P. Turq, G. Gebel, R. Kahn, A. Vandais, J.-P. Noel, C. Malveau, D. Canet, J. Phys. Chem. B 105 (2001) 4503.
[15] A.-L. Rollet, M. Jardat, J.-F. Dufreche, P. Turq, D. Canet, J. Mol. Liquids 92 (2001) 53.
[16] A.A. Gronowski, H.L. Yeager, J. Electrochem. Soc. 138 (1991) 2690.
[17] S.J. Paddison, R. Paul, T.A. Zawodzinski, J. Electrochem. Soc. 147 (2000) 617.
[18] A. Vishnyakov, A.V. Neimark, J. Phys. Chem. B 105 (2001) 9586.
[19] M.R. Tarasevich, A. Sadkowski, E. Yeager, in: B.E. Conway, J.O'M. Bockris, E. Yeager, S.U.M. Khan, R.E. White (Eds.), Comprehensive Treatise of Electrochemistry, vol. 7, Plenum Press, New York, 1983, pp. 301–398.
[20] P.C. Foller, R.T. Bombard, J. Appl. Electrochem. 25 (1995) 613.
[21] P. Piela, P.K. Wrona, J. Phys. Chem. B 105 (2001) 1494.
[22] F. Aziz, G.A. Mrza, Talanta 11 (1964) 889.